minerals

MDPI

Article

The Significance of Metasomatism in the Formation of the Tanbreez REE Deposit in South Greenland

Hans Kristian Schønwandt [1], Thomas Ulrich [2,*], Greg Barnes [1] and Ole Christiansen [1,3]

[1] G. B. Barnes & Associates, South Perth, WA 6151, Australia; hans.kristian.v.s@gmail.com (H.K.S.)
[2] Institute of Geotechnology and Mineral Resources, Clausthal University of Technology, 38678 Clausthal-Zellerfeld, Germany
[3] Ujarak Aps, 8300 Odder, Denmark
* Correspondence: thomas.ulrich@tu-clausthal.de

Abstract

The layering of the lower layered kakortokite in the per-alkaline Ilímaussaq complex has been interpreted as an orthocumulus rock. Petrographic observation and mineral chemical data from the topmost and the lowest part of the layered kakortokite show signs that indicate massive metasomatic overprint. The occurrence of globular structures in the top part of kakortokite and fine-grained inclusions in the lower layered kakortokite are interpreted as the precursor of kakortokite and the result of a subsolidus reaction between a fluid phase and the underlying rock, respectively. Two different processes led to the formation of kakortokite, a precursor where a clear repetitive layering occurs and a chemical reaction between a fluid phase and the underlying rock where different kakortokite types are randomly interstratified. Both metasomatic events led to a higher rare earth element (REE) grade of the original REE mineralization.

Keywords: kakortokite; metasomatism; REE mineralization; Ilimaussaq; Greenland

Academic Editors: Argyrios Papadopoulos, Panagiotis Voudouris and Constantinos G. Mavrogonatos

Received: 12 June 2025
Revised: 24 July 2025
Accepted: 24 July 2025
Published: 29 July 2025

Citation: Schønwandt, H.K.; Ulrich, T.; Barnes, G.; Christiansen, O. The Significance of Metasomatism in the Formation of the Tanbreez REE Deposit in South Greenland. *Minerals* **2025**, *15*, 797. https://doi.org/10.3390/min15080797

1. Introduction

Kakortokite represents the lowermost exposed member of the magmatic stratigraphy of the Mesoproterozoic IlÍmaussaq complex, South Greenland (Figure 1). Kakortokite is a per-alkaline nepheline syenite with eudialyte s.s. as a rock forming mineral which classifies kakortokite as an agpaitic rock [1,2]. The rock-forming mineral eudialyte contains the commodities zirconium, niobium, tantalum and rare earth elements. This has led the mineral industry to define kakortokite as a deposit for these commodities [3]. The deposit is known as the Tanbreez deposit, which is an acronym for the commodities of the deposit (Ta-Nb-REE and Z(r)).

Drill core data indicate that kakortokite rests on an underlying tephri-phonolite, which is at least 200 m thick. Kakortokite is traditionally subdivided into three parts: (1) A lower layered kakortokite (LLK), (2) a slightly layered kakortokite (SLK) and (3) a transitional layered kakortokite (TLK) [4–6]. Recently it has been suggested to reconsider this division and only define LLK and SLK, because the most prominent layering in TLK can be attributed to metasomatic processes [3].

The iconic layering of LLK consists of three-layered units composed of a black, red and a white layer caused by variation in modal amounts of arfvedsonite, eudialyte and feldspar-nepheline, respectively. It is agreed on that kakortokite of LLK is an orthocumulus rock in which the principal cumulus minerals are feldspar-nepheline, arfvedsonite and eudialyte.

However, the formation of the macro rhythmic layering of the LLK is highly debated and several processes have been suggested. An overview of the proposed processes together with relevant references can be found in, e.g., [2,7–10].

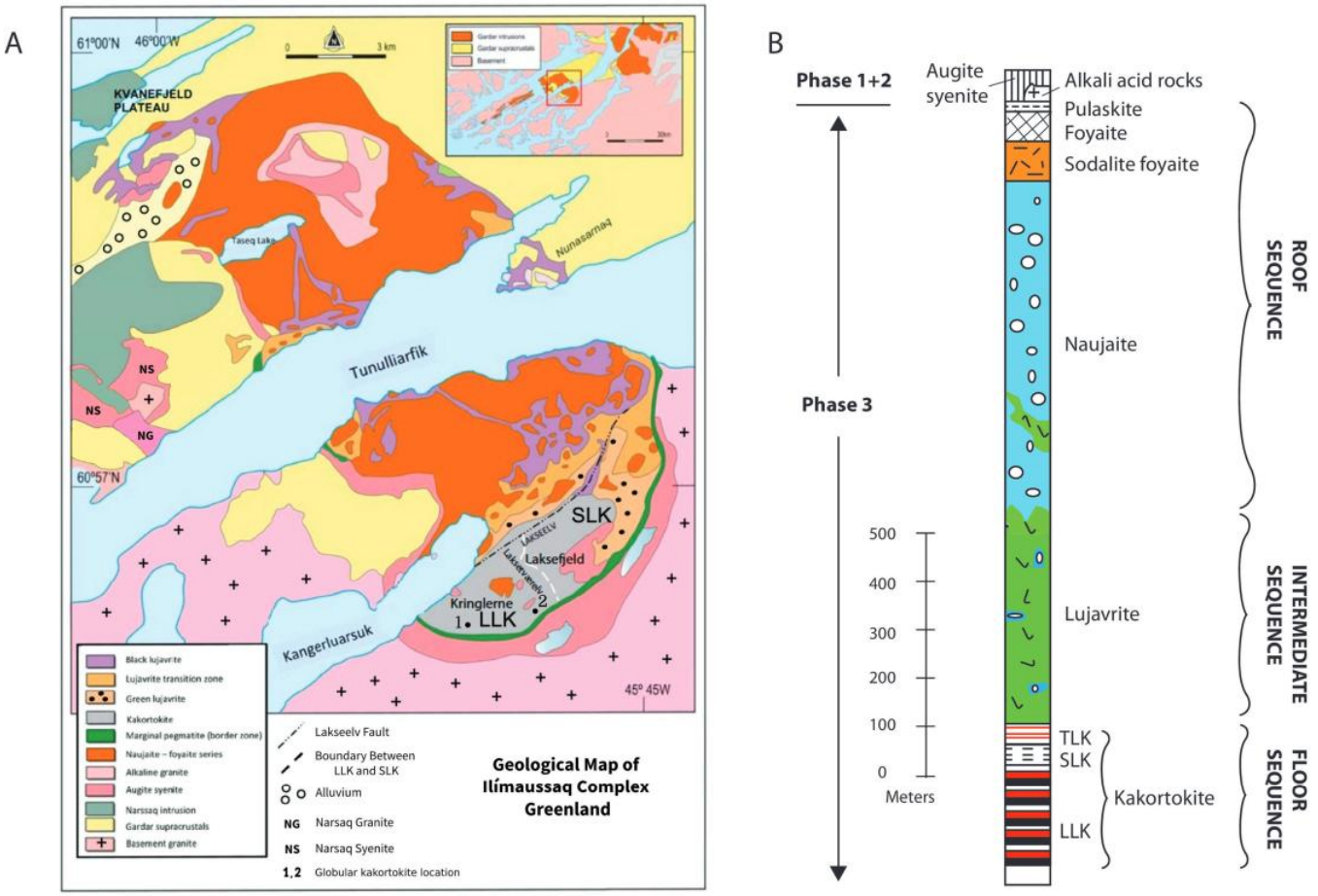

Figure 1. (**A**) Geological map of the Ilímaussaq complex (modified from [3], which was based on [11,12]. Boundary shown between LLK and SLK is based on the numbering of the layers of LLK and the absence of numbering in the SLK on the geological map [12]. Samples from kakortokite in drill cores used in this study are from drill core 24-B, 24-K and 24-X that are located in the SW corner of the intrusions, close to the marginal pegmatite. (**B**) Schematic stratigraphic section through the Ilímaussaq complex, modified from [11,13].

Our study presents new petrographic observations of textures and rock inclusions in the lower layered kakortokite (LLK) that have not been documented before. In the upper part of LLK there are globular (weathering) structures, and in the lower most part of LLK rock inclusions can be found. Both features are investigated here in terms of petrography, mineralogy, and geochemistry. Our interpretation leads to the suggestion that parts of the LLK have been formed by metasomatic processes. The globular structures are interpreted as evidence that the upper part of LLK had a precursor involved in its formation. The inclusions in the lower most part of LLK are the result of a reaction between a peralkaline fluid phase and the underlying tephri-phonolite. Therefore, the origin of the lower layered kakortokite as a pure orthocumulus sequence is questioned, and a metasomatic cause for the formation of part of the lower layered kakortokite is suggested.

2. Geological Setting

The Ilímaussaq intrusive complex belongs to the Mesoproterozoic (1600–1000 Ma) Gardar province in South Greenland. The Gardar province represents a failed continental rift

and consists of sandstone, alkaline volcanic and plutonic rocks, of which several are peralkaline intrusive complexes [7]. The Ilímaussaq complex has been dated at 1160 ± 5 Ma [14] and 1156 ± 1.4 Ma [10] and is among the youngest intrusions of the Gardar province.

The Ilímaussaq intrusive complex is 17 × 8 km in size and at least 3 km thick (Figure 1, [11,12]). It largely comprises alkaline to peralkaline felsic rocks and many of them are agpaitic (bulk rock chemistry molar (Na + K)/Al ≥ 1.2) and contain eudialyte-group minerals (Sørensen, 1997 [1]; Marks et al., 2020 [15]). The development of the Ilímaussaq intrusive complex has been described as a succession of at least three magmatic pulses that crystallized at about 3–4 km depth [12,13,16–20]. In this contribution we have investigated samples from the lower layered kakortokite (LLK), which is the lowermost exposed part of the intrusion.

3. Sampling and Analytical Methods

The samples were collected from field outcrops of the topmost unit (Figure 2) in the lower layered kakortokite as well as from drill cores that penetrate the lithology just below the kakortokite.

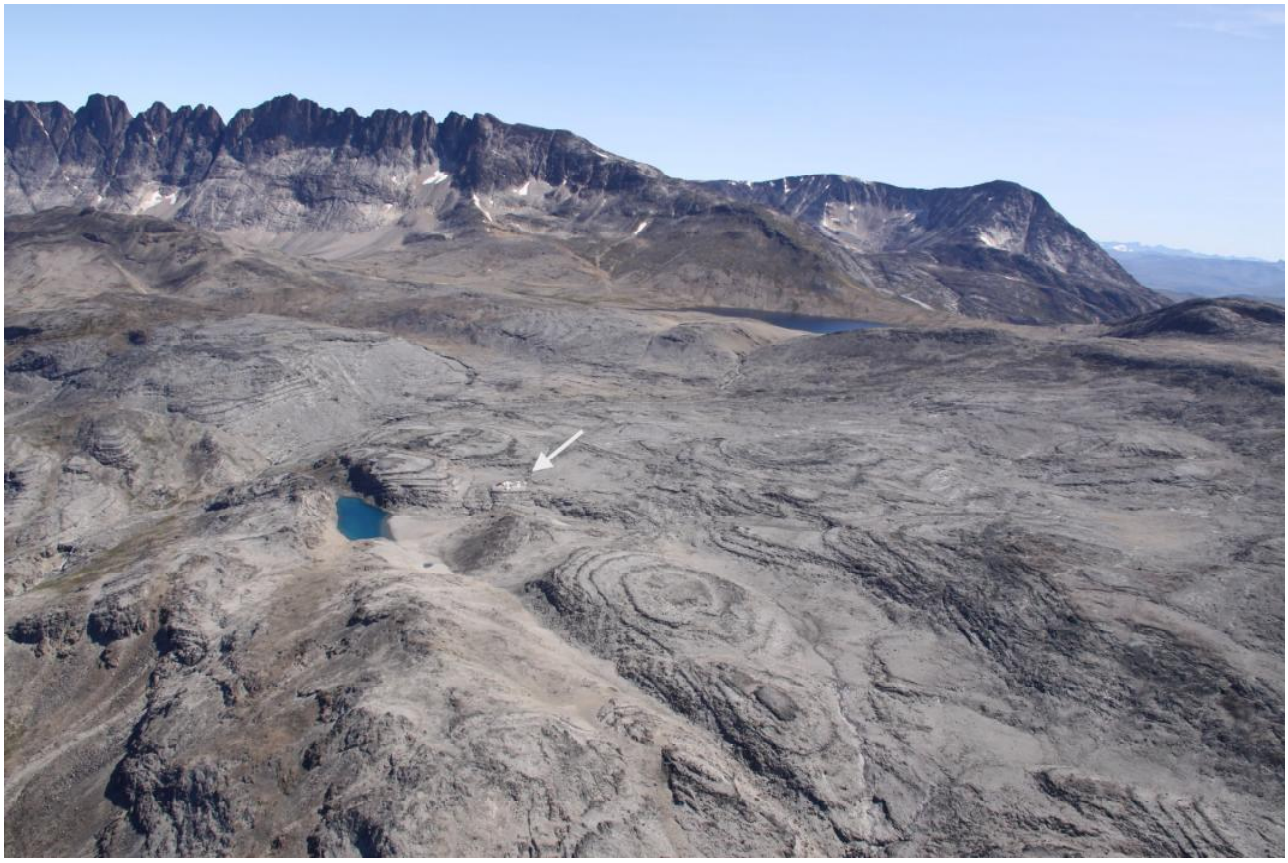

Figure 2. Aerial view of lower layered kakortokite. Arrow indicates drilling camp.

Polished thin sections were prepared and investigated with an Eclipse 600 polarization microscope from Nikon, Tokyo, Japan to describe the textures and modal compositions. Selected samples were then analyzed by electron microprobe. At the Department for Geoscience, Aarhus University, Aarhus, Denmark, using a JEOL (Toky, Japan) JXA-8600 Superprobe and at Clausthal University of Technology, Clausthal-Zellerfeld, Germany, using a Cameca (Gennevilliers, France) SX5 microprobe. Backscatter electron images (BSE) and energy-dispersive spectrometry were used to determine the composition of the feldspars, nepheline, aegirine, arfvedsonite, and eudialyte. The analytical conditions were

15 kV energy, 10 nA current, and a beam size of about 5 µm. Mineral and synthetic standards (MgO (Mg), corundum (Al), quartz (Si), rutile (Ti), albite (Na), orthoclase (K), apatite (Ca, P), tugtupite (Cl), zircon (Zr), monazite (REE), hematite (Fe)) were used for the calibration. The analysis quality was monitored with in-house standards (labradorite plagioclase).

4. Sample Description and Petrography

The type locality for kakortokite is the Kringlerne area on the south side of Kangerluarssuk [21] (Figure 1). Bohse et al. [4] mapped and established a terminology for the sequence, which consists of black, red and white horizons, each of which is termed a layer. This three-colored layering, which is repeated up through the stratigraphy, forms the iconic rhythmically layered kakortokite and makes up the LLK [4,5]. The sequence of three layers (black, red, white) has been termed a "unit". A prominent unit along the Kringlerne cliff was chosen as a reference in the mapping and is known as unit 0. A total of 29 units has been mapped equivalent to a thickness of 212 m. Seventeen units occur above the reference unit and eleven below, leading to the labelling of +1 to +17 and −1 to −11, respectively [4]. In the Kringlerne area the topmost unit with significant outcrop is unit +16, whereas unit +17 only occurs as small erosional remnants.

In the upper part of the kakortokite sequence in the Kringlerne area (Figure 1, locality 1) there are peculiar weathering features visible. Here, the kakortokite shows globular structures and weathers out as several centimeter-sized 'balls' (Figure 3). This weathering feature appears in a horizon and is about 1 m thick and can be followed for more than 10 m and is best characterized as an eudialyte-rich white kakortokite (Figure 3). There is a gradual change from a weakly foliated eudialyte-rich kakortokite (Figure 4A) over to a kakortokite that locally shows globular structures (Figure 4B) to a kakortokite that consists of up to 90% of these structures (Figure 4C), weathering out as a regolith consisting of globular-structured kakortokite (Figures 3 and 4D).

Another location where this weathering structure has been observed occurs also in the upper part of the LLK sequence, but approximately 1.5 km east of the first location (Figure 1, locality 2). The globules here are smaller, about 3 cm in diameter (Figure 5) and occur in loose blocks of local origin. Similarly to the first locality, the globular structure appears to be made of white kakortokite.

Globular shapes in igneous rocks are often referred to as spheroidal, ocelli or orbicular structures. The term spheroidal also imply that the structure consists, e.g., of radiating minerals or is made up of a core surrounded by rings with slightly different modal composition [15] whereas orbicular will refer to concentrical layers of different modal composition. The globular structure found in kakortokite does not have this type of affiliation; therefore, we use the term globular kakortokite.

When the globular structures are cut in half is a feldspar porphyritic texture with scattered eudialyte can be observed (Figure 5C). The matrix is leucocratic to mesocratic with centimeter long, subparallel feldspar megacrysts. The megacrysts appear as perthite and represent about 20% of the globules (Figure 5C).

Only the outer edge (≈1 mm thick) of the globular structure is dominated by feldspar-nepheline, which resembles that of a white kakortokite (Figure 5C). At a few places along the outer edge of the globules, there are domains dominated by feldspar-nepheline that penetrate the globules (arrows in Figure 5C). The smaller globular structures from locality 2 show a corresponding texture but with a more prominent feldspar replacement of the matrix than in the larger globules (Figure 5A).

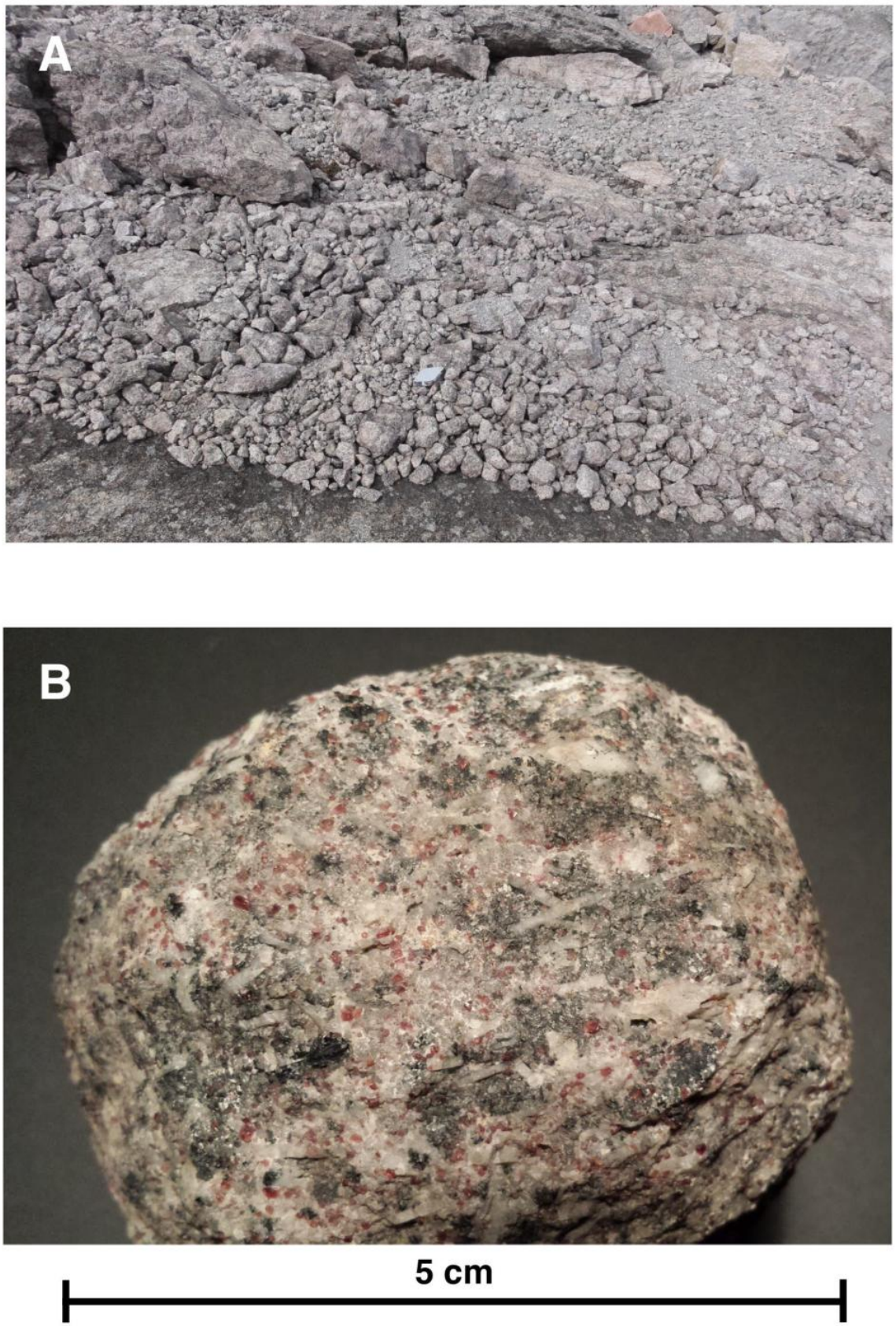

Figure 3. (**A**) Regolith of globular-structured kakortokite. Hand lens for scale (8 cm). (**B**) Single globule, 8 cm in diameter from locality 1 (Figure 1).

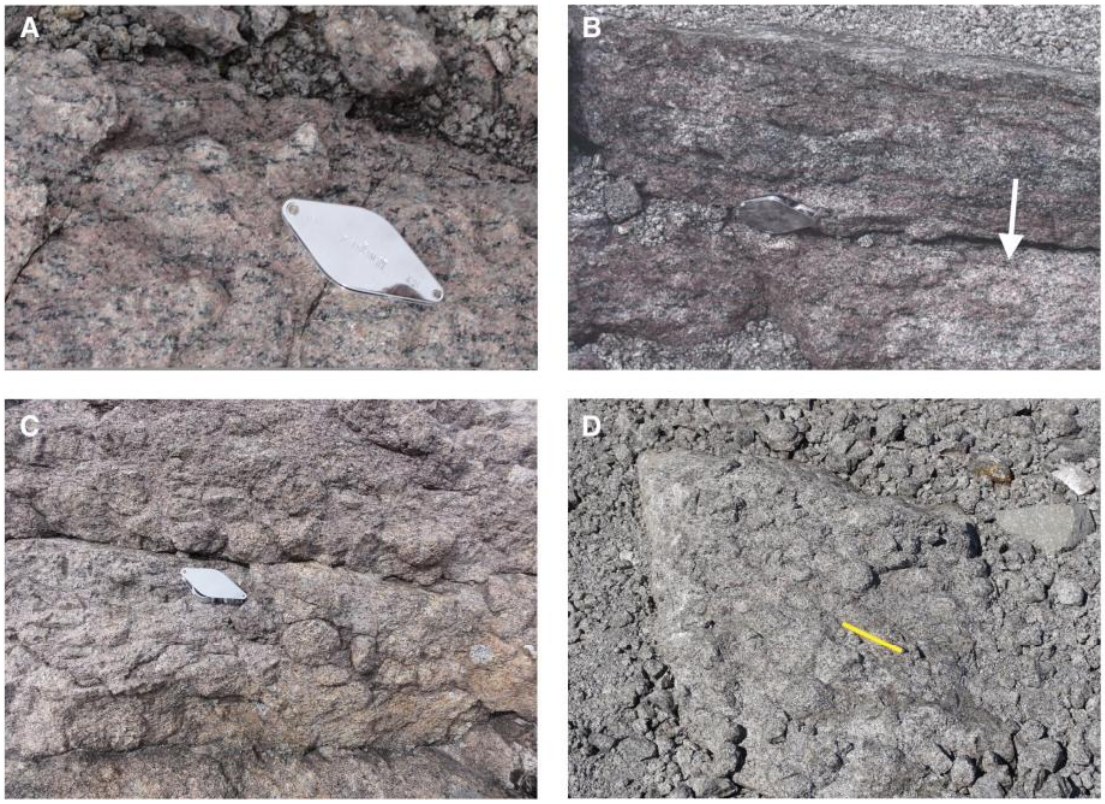

Figure 4. (**A**) Eudialyte-rich white kakortokite without globular structure. (**B**) Eudialyte-rich white kakortokite with a few globular structures, arrow indicate a globular structure. (**C**) White kakortokite dominated by globular structures. Hand lens for scale (8 cm). (**D**) Kakortokite dominated by globular structures surrounded by regolith of globular kakortokite. Hand magnet for scale, 10 cm.

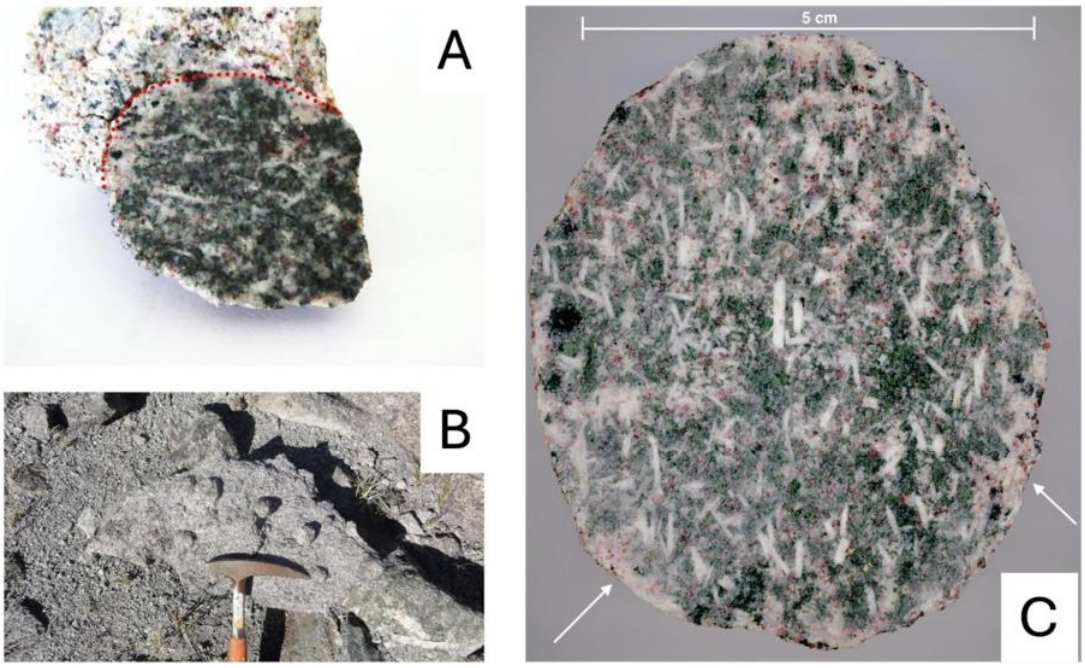

Figure 5. (**A**) Cut open single globule from locality 2 (Figure 1). Diameter 4 cm. (**B**) Occurrence of globular structured kakortokite from locality 2 (Figure 1). (**C**) Cut open globule from locality 1 (Figure 1) showing feldspar porphyry in a fine-grained mesocratic matrix with scattered eudialyte. Domains of feldspar-nepheline (arrows) penetrate the globule.

The perthite megacryst laths show the same intimate intergrowth of microcline and albite as described by [22] (Figure 6). Microcline does not show the typical cross-hatched twinning but appears as an irregular penetrative twinning following the albite law with (010) as twinning plan [21,23]. The albite-rich parts of the perthite laths show fine polysynthetic twins elongated parallel to (010) of the perthite laths and exhibits a close intergrowth with the microcline part of the laths (Figure 6).

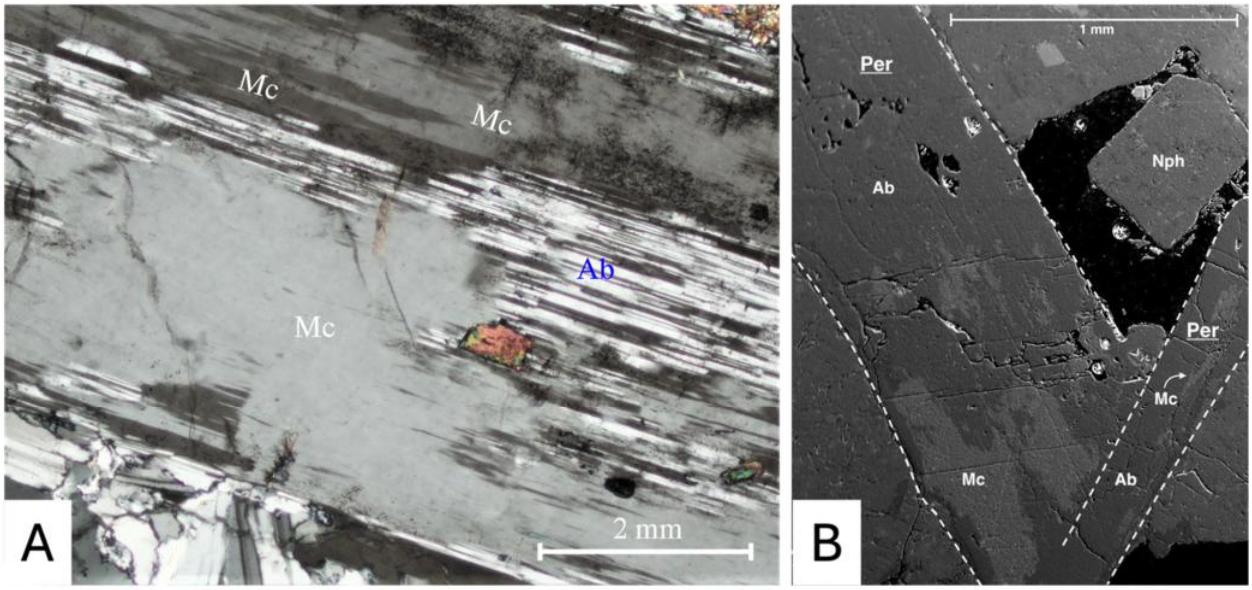

Figure 6. (**A**) Thin section of perthite megacrysts showing intimate intergrowth of microcline (Mc) and polysynthetically twinned albite (Ab) (lower part of figure). The microcline in the center is between extinction positions where twin individuals appear as optical homogenous. Upper part of figure shows an individual with irregular penetrative twining following the albite law with (010) as twining plan. XPL black (Mc) individual in extinction position. (**B**) BSE image of perthite lath (Per) showing extensive albite (Ab) replacement resulting in microcline (Mc) inclusions in albite. Nph: nepheline.

The perthite laths vary in composition from 20% albite and 80% microcline to nearly 100% albite. In the albite dominated grains microcline occurs as inclusions in the central part of the individual laths and exhibits a variety of shapes from threaded outline elongated parallel to the length of the lath (Figure 6) to irregular and lobed inclusions.

The perthite megacryst laths grow onto the matrix, which locally results in nepheline and eudialyte inclusions in the megacrysts. Eudialyte retains its euhedral shape in the perthite laths (Figure 7), whereas nepheline occurs as lobed grains in the megacrysts. Locally tiny grains of aegirine occur also as inclusions in the megacrysts.

A few anhedral perthite grains occur in the matrix, having a grain size of about 3–5 mm (Figure 7). These grains are very turbid and are penetrated by veinlets of microcrystalline albite, which also occurs as a lobed ribbon along the boundary of the grains. Despite the turbidity, a tiled structure [24] is locally recognized.

The similarity between the megacrysts of the globules and the perthite laths of kakortokite from LLK indicate, that the globules have experienced the same suggested albitization as described for the lower layered kakortokite, where the microstructures are interpreted as albite replacement (albitization) [25].

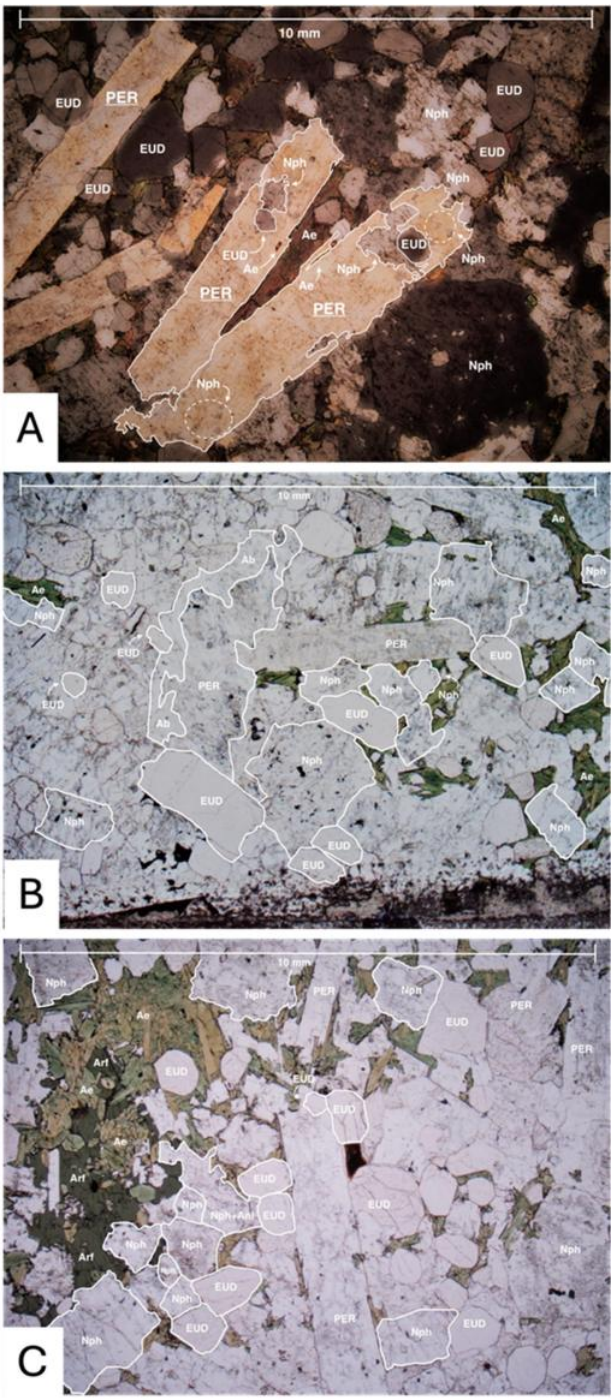

Figure 7. (**A**) Thin section in XPL of perthite laths (Per) in the eudialyte (EUD)-urtite matrix. The boundary of the laths is irregular to such an extent that some of the nepheline (Nph) nearly appears as inclusions (arrows) beyond that, and nepheline occurs as irregular inclusions or as an accumulation of tiny inclusions (circle areas). In contrast, eudialyte inclusions appear to have retained their shape. Aegirine (Ae) inclusions occur in the laths where the neighboring mineral in the matrix is aegirine. (**B**) Thin section in PPL of eudialyte-urtite showing a texture dominated by sub- to euhedral eudialyte (EUD) and nepheline (Nph) with interstitial aegirine (green). Some nepheline occurs with tiny aegirine inclusions. Central part of figure perthite lath (Per) penetrating anhedral perthite, which on the left side is lobed by microcrystalline albite (Ab). (**C**) Thin section in PPL of eudialyte-urtite with perthite laths (Per) that appear with eudialyte (EUD) inclusion and partially enclose aegirine (Ae). The texture is controlled by euhedral eudialyte (EUD) and nepheline (Nph) with some minor anhedral nepheline some of which is altered to analcime (Anl). Aegirine and arfvedsonite (Arf) occur interstitially.

The microstructure of the matrix is hypidiomorphic granular, consisting of eudialyte and nepheline with interstitial aegirine and locally arfvedsonite (Figure 7B,C). Euhedral eudialyte (≈1 mm in diameter) and sub- to euhedral short prismatic nepheline (≈1 mm in diameter) appear as the principal minerals of the matrix, whereas a small portion of nepheline is anhedral and occurs with concave contacts and appears as interstitial grains between the euhedral eudialyte and nepheline (Figure 7C).

Eudialyte in the globular-structured kakortokite shows no alteration nor pronounced sector or concentric zonation, unlike the rest of the eudialyte in the LLK. The anhedral nepheline is bigger (2–3 mm in diameter) in grain size and has several inclusions of aegirine and arfvedsonite compared to the smaller euhedral nepheline, which generally is inclusion-free.

The estimated modal composition of the matrix is 60% nepheline, 20% eudialyte and 20% aegirine.

Plotting the modal composition in the diagram alkali-feldspar (A), nepheline (F) and mafic minerals (color index M') after recalculating alkali-feldspar + nepheline + pyroxene to 100%, classifies the rock to be an urtite [26]. Consequently, the rock with the globular texture can be called a porphyritic eudialyte-urtite.

5. Chemical Mineral Compositions

5.1. Mineral Compositions of the Urtite Alkali-Feldspar Composition

As described above, two types of alkali-feldspar occur. The first type are perthite laths, which appear as megacrysts and show an intimate intergrowth of microcline and albite, while the second type of feldspar is anhedral, lobed and veined by microcrystalline albite.

Microprobe analyses of albite and microcline from both types of alkali-feldspar grains are shown in Table 1. Microcline from perthite laths and the anhedral grains are very similar in composition. They are Na-poor and are like microcline from peralkaline rocks elsewhere [27]. The low contents of Na and Ca allows Na to be in solid solution in microcline [28]. The albitic part of the lath shaped perthite and the microcrystalline albite that crosscuts the anhedral microcline show a very similar composition with exceptionally low Ca-content.

Table 1. Electron microprobe analyses showing average composition of albite and microcline.

	Albite		**Microcline**	
	Perthite	**Microcrystalline Veins**	**Perthite**	**Anhedral Grains**
n	9	2	7	2
SiO_2	67.90	65.46	63.58	62.99
TiO_2	0.02	0.22	0.01	0.14
Al_2O_3	19.63	18.75	18.47	18.21
FeO	0.14	0.25	0.08	0.12
MnO	0.02	0.04	0.04	0.13
MgO	0.03	bdl	0.01	0.02
CaO	0.01	0.09	bdl	bdl
Na_2O	11.38	10.42	0.40	0.45
K_2O	0.44	1.13	17.05	16.72
Total	99.57	96.36	99.87	98.78

n: number of grains analyzed. bdl: below detection limit.

5.2. Eudialyte Composition

Table 2 shows preliminary analyses of eudialyte from globular kakortokite. Further analysis is planned to constrain the composition of eudialyte and any changes in the calculated distribution of elements in the various structural positions. The analyses demonstrate the difference in composition of eudialyte from the globular kakortokite and LLK. Using the composition of eudialyte determined by [8] from the LLK, the eudialyte from globular kakortokite is richer in Na, Mn and Y but it has a lower Si content.

Table 2. Electron microprobe analyses of eudialyte from globular kakortokite. Calculated formula units for Z = 3. Calculation is based on 75 anions.

	Wt%	**Cal. Formula**	**Wt%**	**Cal. Formula**
Number of Grains	**2**		**2**	
Na	12.29	17.00	12.62	17.00
Si	22.04	25.10	21.81	25.00
Zr	8.41	2.95	8.39	3.00
Cl	1.53	1.40	1.53	1.40
Ca	8.31	6.70	8.31	6.70
Ce	0.92	0.20	0.88	0.20
Fe	4.33	2.50	4.25	2.50
La	0.42	0.10	0.40	0.10
Pr	0.10	0.00	0.10	0.00
Nd	0.21	0.00	0.20	0.00
Mn	0.66	0.40	0.65	0.40
Sm	0.05	0.00	0.05	0.00
Y	0.47	0.20	0.47	0.20
H	0.05	1.60	0.05	1.60
O	37.56	75.00	37.38	75.00
Total	97.35		97.10	

Proposed calculated formula: $Na_{17}(Ca, Lanth)_7(Fe{+}{+}, Mn, Y)_3Zr_3Si_{25}O_{73}(OH, Cl)$.

5.3. Nepheline Composition

Nepheline occurs in two varieties: (i) a euhedral to subhedral prismatic form and (ii) as anhedral grains with concave outline. Both types have inclusions of aegirine and arfvedsonite; however, the euhedral grains generally appear with fewer inclusions. Table 3 shows microprobe data of nepheline. The composition of the nepheline is divided into two types. The first is Fe-rich with about 1.6 wt% Fe, and the second is Fe-poor with 0.51 wt% Fe on average. The Fe-rich nepheline has a higher content of SiO_2 than the Fe-poor nepheline, which on the other hand is richer in Al and K. The composition of the nepheline has been calculated based on 24 cations and 32 oxygen. Table 3 shows that both types are homogeneous and that they plot on the kalsilite side of the [29] trend of natural nepheline composition (Barth joint) in the Q-Ne-Ks diagram (Figure 8). This classifies them among the relative rare K-rich nephelines and with a clearly different composition than the rest of nepheline in the Ilímaussaq complex (Figure 8).

Table 3. Electron microprobe analyses of nepheline from globular kakortokite.

Analysis	1	2	3	5	6	7
SiO_2	47.03	47.78	45.52	44.74	47.60	47.00
Al_2O_3	33.25	33.11	34.88	34.67	33.35	33.77
TiO_2	0.02	0.02	0.02	0.01	0.01	0.02
Fe_2O_3	1.62	1.51	0.53	0.49	1.78	1.42
MnO	0.03	0.03	0.04	0.02	0.03	0.02
MgO	0.01	0	0.01	0.01	0.01	0.01
CaO	0.02	0.01	0.06	0.01	0.01	0.01
Na_2O	13.15	13.16	13.27	13.36	12.96	13.38
K_2O	5.65	5.65	6.79	6.68	5.69	5.96
Total	100.78	101.27	101.12	99.99	101.44	101.59
Composition of nepheline						
Ne	68.85	68.01	69.02	69.93	67.98	69.04
Ks	19.46	19.21	23.24	23.01	19.64	20.23
Qtz	11.69	12.78	7.74	7.06	12.39	10.73

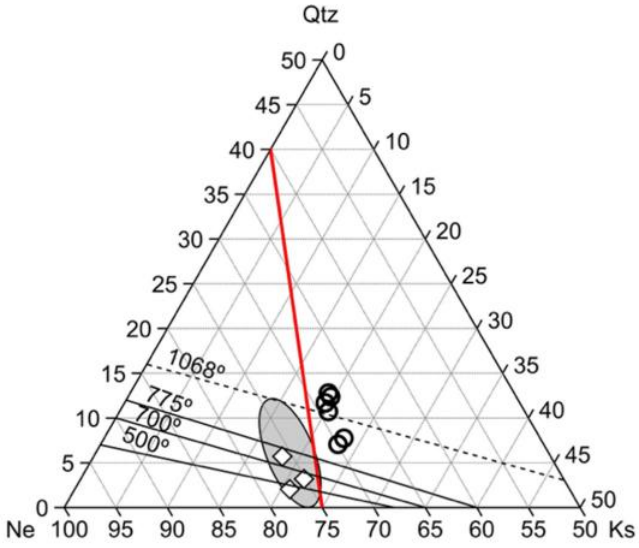

Figure 8. Qtz-Ne-Ks diagram of nepheline composition of eudialyte-urtite. Outlined area shows nepheline composition of sodalite foyaite, naujaite and kakortokite from Ilímaussaq [30]. Open circles are data from this study. Isotherms drawn from [31].

5.4. Arfvedsonite and Aegirine Composition

Representative microprobe data of arfvedsonite and aegirine are shown in Table 4 together with data from the literature from kakortokite. The composition of amphibole is calculated following the IMA recommendations [32] and is based on 23 oxygens, and the pyroxene is calculated according to IMA recommendations [33] based on four cations and 6 oxygens.

Table 4. Electron microprobe analyses of arfvedsonite and aegirine from kakortokite and globular kakortokite.

	Arfvedsonite			Aegirine		
	Kak		Glob Kak	Kak		Glob Kak
	(a)	(b)		(c)	(d)	
SiO_2	45.50	47.20	49.90	52.14	52.74	53.53
TiO_2	1.54	0.61	0.56	0.42	0.95	0.66
Al_2O_3	4.48	2.57	1.88	0.99	1.09	1.14
FeO	31.47	32.94	34.13	28.75	31.82	30.36
MnO	0.66	0.63	0.86	0.11	0.19	0.17
MgO	2.14	0.70	0.81	0.11	0.09	0.07
CaO	3.93	2.28	0.93	2.36	2.22	2.20
Na_2O	6.75	7.75	6.50	12.55	10.44	10.29
K_2O	1.70	1.66	2.70	-	-	-
Total	98.17	96.34	98.27	97.43	100.04	98.42
			Apfu			
Si	7.63	8.09	8.35	1.99	2.01	2.07
Ti	0.19	0.08	0.07	0.01	0.02	0.02
Al	0.89	0.52	0.37	0.04	0.05	0.05
$Fe^{+3}{}_{cal}$	0.00	0.00	0.00	0.88	0.61	0.54
$Fe^{+2}{}_{cal}$	4.41	4.72	4.77	0.04	0.40	0.45
Mn	0.09	0.09	0.12	0.00	0.01	0.00
Mg	0.53	0.18	0.20	0.01	0.01	0.01
Ca	0.71	0.42	0.17	0.10	0.10	0.09
Na	2.19	2.58	2.11	0.93	0.77	0.77
K	0.36	0.36	0.58	-	-	-

(a) Average of six samples from [34]; (b) average of two samples from [35]; (c) assay of one sample from [35]; (d) assay of one sample [30]. Kak: kakortokite; Glob. Kak: globular-structured kakortokite.

The amphibole of the globular-structured kakortokite is classified as a member of the sodic group and the detail categorization is within the group of arfvedsonite.

Following the recommended procedure [33], the pyroxene of globular-structured kakortokite is in the Q-J diagram classed as a Na-Ca pyroxene of the aegirine-augite species.

6. Whole-Rock Chemistry

The appearance of eudialyte-urtite in the LLK sequence (Figures 4 and 5) indicates that it is a possible precursor to white kakortokite. If that is the case, then the amount of perthite must increase from around 20% in the porphyritic eudialyte-urtite to around 50% in white kakortokite.

The porphyritic eudialyte-urtite has an average of 20% perthite and 50% nepheline. In contrast, white kakortokite has a general composition of 50% perthite and 20% nepheline. The change in the ratio of nepheline to perthite is clearly reflected in the bulk rock analyses where high Al and Na + K in porphyritic eudialyte-urtite is matched by significantly lower values in white kakortokite (Table 5). Otherwise, the two rocks show low concentrations of Ti and a high content of Zr compared to other major rock types in the Ilímaussaq Complex (Table 5).

Table 5. Major element analyses of globular kakortokite, tephri-phonolite, and representative rocks from the Ilímaussaq intrusion (in wt%).

Rock	GK	# F	# SF	# N	# WK	T-PH
SiO_2	50.27	58.50	48.24	48.25	53.30	53.41
TiO_2	0.12	0.32	0.33	0.32	0.16	1.46
ZrO_2	1.82	0.27	0.51	0.49	1.30	0.12
Al_2O_3	19.84	16.21	18.99	19.30	13.40	14.79
FeO	6.24	6.53	6.82	6.74	10.53	11.57
MnO	0.14	0.19	0.20	0.21	0.31	0.32
MgO	0.03	0.11	0.12	0.10	0.23	1.39
CaO	1.86	1.76	1.67	1.68	2.10	3.99
Na_2O	14.29	7.56	14.87	14.37	8.84	7.44
K_2O	3.26	5.65	3.47	3.41	4.04	4.16
P_3O_5	0.02	0.04	0.06	0.06	0.04	0.55
Total	97.89	97.14	95.28	94.93	94.25	99.19

GK: Globular kakortokite; T-PH: Tephri-phonolite, average of six samples. F: Foyaite #; SF: Sodalite foyaite #; N: Naujaite #; WK: white kakortokite #. #: Representative analyses from [13].

Table 6 shows the REE content of eudialyte-urtite and white kakortokite. The chondrite-normalized REE patterns are shown in Figure 9 and display a pronounced negative Eu anomaly for the porphyritic eudialyte-urtite and white kakortokite, which generally is assumed to be due to fractionation of large amounts of plagioclase from basaltic magmas and thereby depleting the residual magmas in Eu [34,36]. The steepness of the curves for LREE (La/Sm, chondrite normalized) are very similar for porphyritic eudialyte-urtite and white kakortokite being 4.3 and 4.4, respectively. The HREE (Tb/Lu, chondrite normalized) show a less steep curve reflecting ratios of 1.3 and 1.6 for porphyritic eudialyte-urtite and white kakortokite, respectively. This results in a ratio of La/Yb of 6.5 and 7.7 for porphyritic eudialyte-urtite and white kakortokite, respectively. Moreover, to point out the enrichment of white kakortokite in REE compared to globular kakortokite we have normalized the REE content of globular kakortokite (Table 6). The REE bulk rock content is dominated by the amount of eudialyte in the rock and this can be normalized using the bulk rock ZrO_2 content because eudialyte is the main mineral containing zirconium in these rocks.

Table 6. Analyses of REE in globular kakortokite, white kakortokite and tephri-phonolite.

(ppm)	Glob. kak	White kak [(a)]	Norm. [(b)]	T-Ph [(c)]
Ce	1395	1460	1004	511
La	726	743	523	267
Pr	156	-	112	62
Nd	552	573	397	208
Sm	106	105	76	38
Eu	11	7.18	8	6
Gd	104	-	75	33
Tb	19	21	14	4
Dy	124	-	89	31
Ho	27	-	19	6
Er	82	-	59	18
Tm	12	-	-	3
Yb	76	65.2	55	18
Lu	10	9.2	7	3
Y	600	759	432	163
ZrO_2 (%)	1.82	1.30	1.30	0.12

[(a)] Representative analyses from [13]; [(b)] normalized REE content in globular kakortokite according to Zr02; [(c)] average of 6 samples. -Not analyzed.

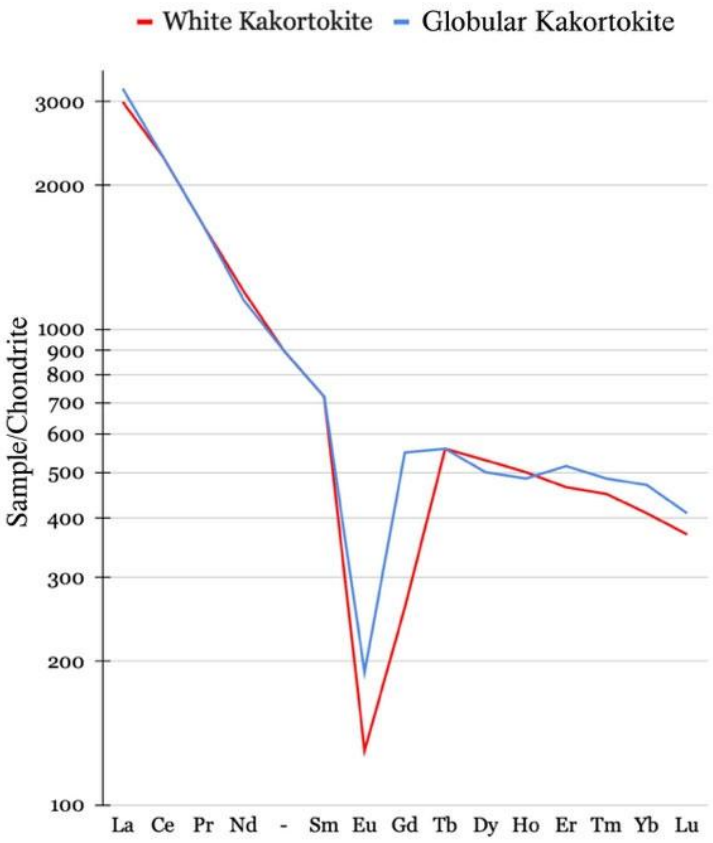

Figure 9. Chondrite-normalized REE distribution of white kakortokite and globular-structured kakortokite. Chondrite values from [37].

The modal composition of the globular kakortokite indicate that it is a new rock type in the Ilímaussaq complex. This is supported by the fact that the main minerals (nepheline and eudialyte) differ also compositionally from corresponding minerals in the Ilímaussaq complex. Eudialyte-urtite represents a new agpaitic rock type in the Ilímaussaq complex.

7. Inclusions in the Lower Layered Kakortokite

The contact between the kakortokite and the underlying tephri-phonolite is sharp and encountered in boreholes about 20 m below sea level in the coastal area south of Kangerluarsuk.

In the boundary zone between kakortokite and tehpri-phonolite tephri-phonolite appears as inclusions in kakortokite, and correspondent veins of kakortokite occur in tephri-phonolite. The border between the two rocks is set where kakortokite, e.g., is replaced by tephri-phonolite as the dominant rock. The boundary can usually be determined within 25–50 cm. The boundary zone is a general phenomenon and occurs from the outer augite syenite and into the central part of kakortokite (Figure 1).

In the boundary zone the typical black, white and red kakortokite members are no longer present. Instead, some of the kakortokite looks more mesocratic (i.e., between white (leucocratic) and black (melanocratic) kakortokite). Equally, there is a common type of kakortokite in the boundary zone that consists of eudialyte and arfvedsonite in varying amounts and with accessory feldspar. This type has been termed red-melanocratic kakortokite and is an eudialyte-rich type of kakortokite. Red-melanocratic and red kakortokite often appear spatially together and occur most frequently close to the border with tephri-phonolite. However, the two eudialyte-rich kakortokite occur also higher up in the kakortokite stratigraphy where they appear interstratified with mesocratic or leucocratic kakortokite.

The kakortokite sequence of the boundary zone is characterized by a random mixture of the various types of kakortokite (leucocratic, mesocratic, melanocratic, red-melanocratic and red) and differ significantly from the general description of the kakortokite stratigraphy [4,7,17] that is found in outcrops.

The various types of kakortokite in the boundary zone are characterized by fine-grained (≈0.2 mm), mesocratic inclusions (Figure 10) consisting of arfvedsonite, feldspar, nepheline and aenigmatite with minor amount of rinkite and sodalite. The inclusions are generally of cm size, but inclusions up to 10 cm in diameter occur. The big inclusions generally appear with more coarse-grained (≈0.5 mm) domains and about 10% melanocratic, glomerophyric megacrysts (Fe-rich mica) with a diameter of up to 2 mm.

The inclusions often show concave boundaries towards kakortokite, which otherwise is well defined without being sharp (Figure 10). There is no visible sign of chemical reaction between the inclusions and kakortokite. Locally a small zone of tiny mesocratic inclusions in kakortokite occur along the contact to the inclusion (Figure 10C). The inclusions appear without strain shadow or wrapping of kakortokite minerals around them. The microstructure of kakortokite is unaffected by the inclusions.

The inclusions are more abundant close to the contact with the tephri-phonolite but disappear about 50 m up in the stratigraphy where kakortokite appears more regular without appearing as a clear repetitive sequence. The mesocratic inclusions have the same mineral content and petrographic arrangement including the glomerophyric megacrysts as the underlying tephri-phonolite.

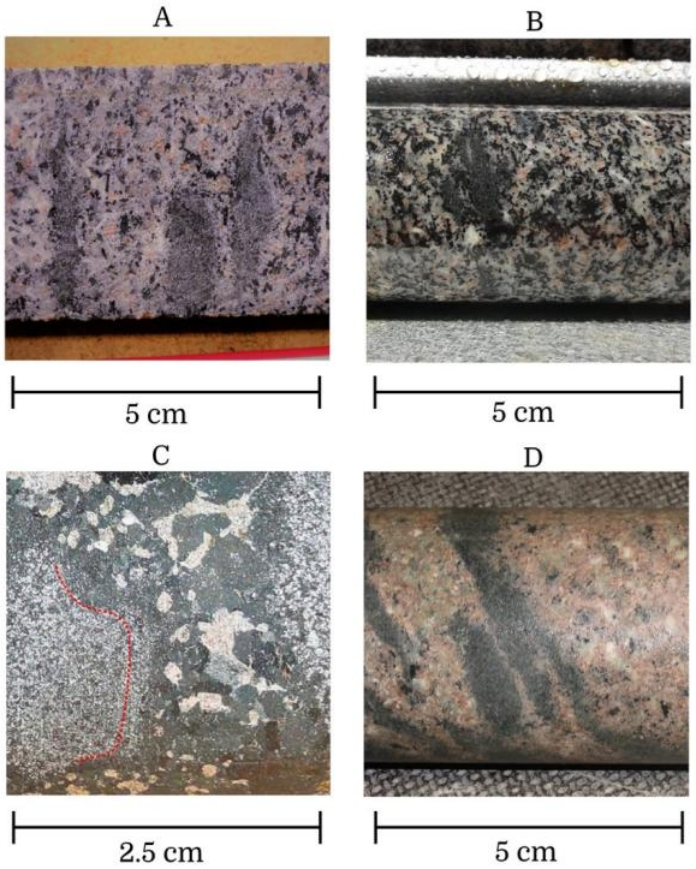

Figure 10. Occurrence of fine-grained inclusions in the various types of kakortokite in the boundary zone. Inclusion in leucocratic kakortokite from drill hole 10-7 (**A**), mesocratic kakortokite from drill hole 24-K (**B**), red-melanocratic kakortokite from drill hole 24-X (**C**), note the zone of very fine-grained inclusions along the boundary between inclusion and kakortokite indicated by the red dotted line. Red kakortokite from drill hole 24-B (**D**).

The occurrence of the fine-grained inclusions in all the various types of kakortokite indicate that the formation of the inclusions is an important aspect in understanding the development of the boundary zone. Figure 11 shows what the initial step in the formation of the inclusions presumably looked like. Veinlets of arfvedsonite and minor eudialyte penetrate and almost surround tephri-phonolite. Besides the replacement of tephri-phonolite by veining, a metasomatic replacement by disseminated eudialyte occurs locally. That replacement appears in loped, cm-sized domains that look slightly more leucocratic and coarser grained than tephri-phonolite (Figure 11C). Eudialyte in these domains appears with an irregular outline; however, a minor part occurs as euhedral grains as in the neighboring red-melanocratic kakortokite. The disseminated eudialyte also occurs in smaller, not particularly well-outlined domains (≈1 cm in diameter) (Figure 11D), which appear scattered in some sections of tephri-phonolite. Both types (vein and disseminated type) occur close to the boundary of tephri-phonolite-kakortokite.

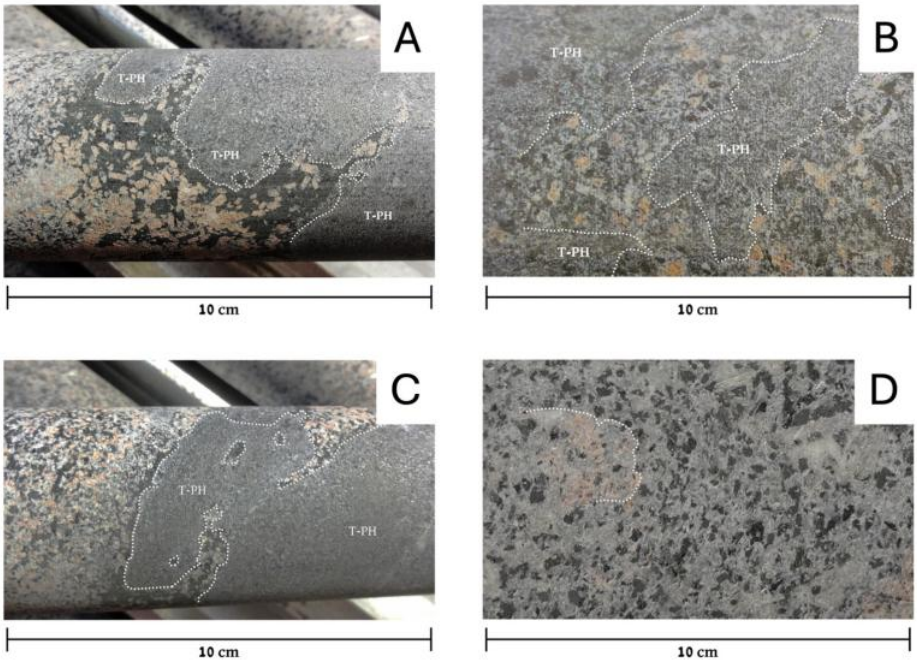

Figure 11. Close up of cores from drill hole 24-X showing the initial stages of formations of the fine-grained, mesocratic inclusions in kakortokite. (**A**) Veinlets of arfvedsonite and minor eudialyte penetrates tephri-phonolite (T-PH) and nearly forms an inclusion. (**B**) Shows loped domains in tephri-phonolite (T-PH) where eudialyte generally appears with irregular outline from drill core 24-X. (**C**) Expansion of the veinlets is shown in (**A**) which also shows that eudialyte becomes more abundant away from the contact indicating that eudialyte in the further process replaces arfvedsonite. Ultimately, red kakortokite can be formed of which an early stage is seen in the lower part of (**A**). (**D**) Smaller domains not very well delimited with diffuse outline of eudialyte from drill core 24-K.

On microscopic scale, evidence for metasomatism is given by the partly resorbed rinkite in the tephri-phonolite (Figure 12A) and new eudialyte is formed, showing convex contact to the tephri-phonolite (Figure 12B). Moreover, the grain size in the kakortokite is much coarser than in the tephri-phonolite.

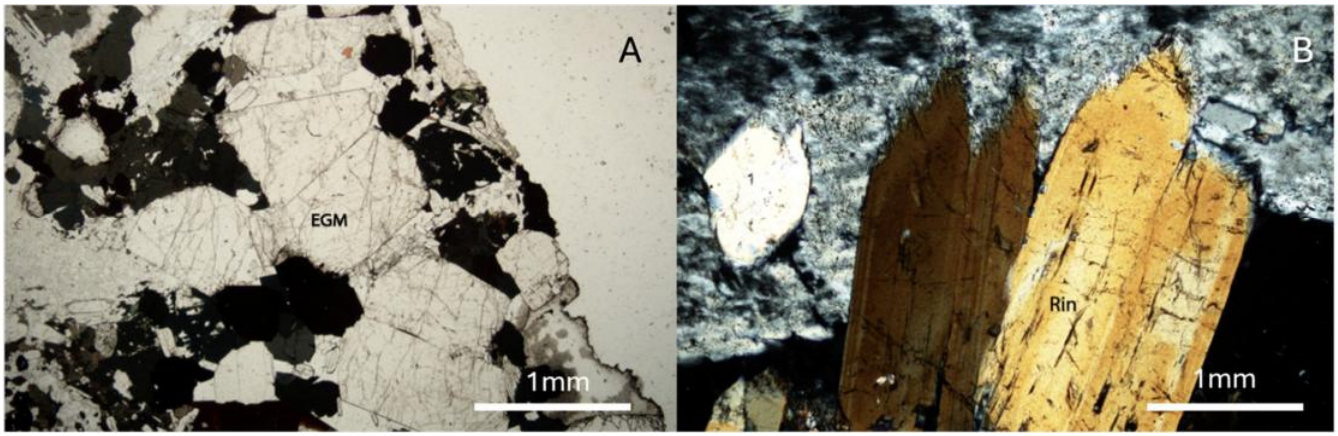

Figure 12. (**A**) Euhedral new eudialyte in coarse-grained kakortokite (PPL). (**B**) Resorbed (irregular crystal surfaces) rinkite in tephri-phonolite indicating dissolution and metasomatism (XPL). EGM: Eudialyte group mineral, Rin: rinkite.

8. Discussion

Our study shows that deviant kakortokite structures are found in the upper part as well as in the lower part of the lower layered kakortokite.

Below we will first discuss the significance of the globular structure and inclusions on the origin of kakortokite, and then some new implications from our observations.

8.1. Globular-Structured Kakortokite

The globular-structured kakortokite occurs on a regional scale (Figure 1) and consists of a perthite porphyritic eudialyte-urtite. The regional spread of this structure suggests that we are dealing with a general phenomenon and, therefore, is of central importance for understanding the formation of kakortokite. The surface of the structure is characterized by the mineral assemblage feldspar-nepheline, which penetrates the globular structure (Figure 5). This shows that this penetration of the eudialyte-urtite can transform the globular structure into white kakortokite.

The perthite megacrysts in eudialyte-urtite are recognized by their inclusions of eudialyte, nepheline and aegirine. Perthite laths show locally irregular contacts to the mineral grains in the matrix. Some of the contacts are so extensive and irregular to the extent that the mineral grains of the matrix, such as nepheline in Figure 7, almost appear as inclusions. This explains the lobed shape of the nepheline inclusions in the perthite laths (Figure 6) and indicates that perthite laths are replacing nepheline of the matrix. Bands and areas of small inclusions of nepheline and aegirine along the outer edge of the perthite laths further support a replacement process. The small mineral inclusions in the perthite laths are identical to the minerals occurring in the matrix (Figure 7). This texture is a common feature of metamorphic rocks where porphyroblasts grow in solid rocks and can lead to a minor part of the replaced minerals being preserved as inclusions [38,39]. Consequently, the perthite laths of the eudialyte-urtite are porphyroblasts. Nepheline and aegirine inclusions represent residuals in the perthite porphyroblasts because they were surpassed by the growth of the perthite since the diffusion rates in nepheline and aegirine are slow, compared with the growth rate of the porphyroblast (perthite) [38]. In contrast, eudialyte keeps its euhedral shape and acts inert to the replacing process in a similar way as suggested for zircon [38]. The similarity in texture of the perthite laths in the globular-structured and the rest of the kakortokite from the LLK indicates that they have been exposed to the same albite replacement as described by [25]. A significant argument for replacement is based on the large variation in composition of the perthite laths regarding albite and microcline. Hypersolvus perthite acts as a nearly closed chemical system regarding exsolution [28], which will result in a minor variation in composition of perthite grains. Therefore, the perthite laths showing large compositional variation cannot be related to exsolution but are best explained by replacement [25]. Originally the perthite laths grew as K-feldspar grains and were later partly replaced by albite. The anhedral perthite grains, which contrary to perthite laths show tiled structure [24], do not have inclusions of the type seen in the perthite laths. Because of the tiled structure and lack of inclusions, a different origin of the anhedral perthite and the perthite laths is indicated. This means that the anhedral perthite most likely would be an original part of the matrix of the eudialyte-urtite. The texture of the eudialyte-urtite supports the assumption that is further underlined by the fact that the perthite lath penetrates the anhedral perthite (Figure 7).

Schønwandt et al. [25] describe the same two structurally different types of perthite from the lower layered kakortokite sequence. They point out that there are no petrographic indications that they represent different stages in the development of kakortokite. However, the replacement stage represented by eudialyte-urtite indicates that the two types of perthite each have their own history of formation and that the tiled structured perthite is not a porphyroblast. Therefore, the tiled structured perthite in kakortokite is most likely a preserved mineral from a precursor which could be eudialyte-urtite. That could explain the

presence of the two perthite types in kakortokite and consequently indicate a metasomatic origin of white kakortokite.

The structural and textural indications that eudialyte-urtite is a precursor to kakortokite in the lower layered kakortokite is supported by the geochemistry of the porphyritic eudialyte-urtite. The chondrite-normalized REE patterns for white kakortokite and eudialyte-urtite (Figure 9) show a similar steepness of the curves for LREE but a less steep curve for eudialyte-urtite regarding HREE. This results in a ratio of La/Yb of 6.5 and 7.7 for porphyritic eudialyte-urtite and white kakortokite, respectively. The ratio La/Yb increases with the evolution of the rocks in the Ilímaussaq complex [13], which gives the eudialyte-urtite a more primitive geochemical signature than white kakortokite. The most striking difference in mineral composition between the eudialyte-urtite (globular-structured kakortokite) and kakortokite occurs in nepheline. In the eudialyte-urtite two kinds of nepheline occur, and both are K-rich; in contrast only one type of nepheline occurs in kakortokite, and they have a composition on the nepheline side of [29] the trend of the natural nepheline (Figure 8). In the Macro-unit II of the Lovozero massif (Layered complex), there are also two types of nepheline, which show a similar difference in composition as those of the eudialyte-urtite [40]. In Lovozero, there is a clear petrographic difference between the two nepheline types as a high content of SiO_2 and Fe_2O_3 occurs in the inclusion-free nepheline, whereas the inclusion rich nepheline is more K-rich and contains less SiO_2 and Fe_2O_3. Both types of nepheline in eudialyte-urtite have inclusions, and this manifests itself in the composition of nepheline, where the difference in SiO_2 and Fe_2O_3 content between the two types is smaller in eudialyte-urtite than in the Lovozero's nepheline. The isotherms in Figure 8 are drawn according to [30] and show a difference in crystallization temperature of about 100 °C between the two types of nepheline in eudialyte-urtite. The crystallization temperature of the anhedral and Fe- and Si-poor nepheline is about 900 °C.

Despite the similarity in composition of nepheline from eudialyte-urtite and Lovozero massif it does not apply for pyroxene (aegirine-augite to aegirine) and amphibole (arfvedsonite) as the Lovozero minerals are significantly more Mg-rich than the ones in eudialyte-urtite. The amphibole and pyroxene in kakortokite show zonation from core to rim reflecting a solid solution from katophorite to arfvedsonite and aegirine-augite to aegirine, respectively [30,41]. The composition of amphibole and pyroxene in eudialyte-urtite occurs with the same rage in compositions and can therefore be considered like the kakortokite minerals.

As the perthite laths of white kakortokite have no or few inclusions of eudialyte and nepheline compared to the perthite lath of eudialyte-urtite, a recrystallization is necessary to establish the texture of white kakortokite. As no signs of deformation occur in the eudialyte-urtite, the recrystallization would be a static adjustment to the physicochemical conditions that have been imposed on the rock. A memory of the original composition of the minerals may be found in some of the minerals in eudialyte-urtite. Despite the fact that white kakortokite suggests having a precursor in the form of eudialyte-urtite, this relationship cannot be extended to include, e.g., black kakortokite, as arfvedsonite of this rock shows no signs of feldspar replacement or recrystallization, which transformed eudialyte-urtite to white kakortokite. Black kakortokite may represent part of the original layering together with eudialyte-urtite. The prominent occurrence of the black kakortokite (Figure 2) could reflect an original magmatic structure. Because the composition of the mafic minerals in kakortokite and eudialyte-urtite are similar, this indicates that both represent the original layering.

8.2. Mesocratic Inclusions

A random mixture of different types of kakortokite, which all occur with fine-grained, mesocratic inclusions, characterizes the boundary zone between lower layered kakortokite and the underlying tephri-phonolite. The presence of mesocratic inclusions in all types of kakortokite indicate that the formation of these inclusions is important for understanding the development of the boundary zone. Figure 11 illustrates the initial stages in the formation of inclusions where veinlets of arfvedsonite and minor eudialyte penetrate tephri-phonolite and nearly surrounds it (Figure 11C). An enlargement of the veinlets caused by chemical reactions between a fluid phase and tephri-phonolite generates the inclusion. It appears from Figures 10C and 11A that arfvedsonite at the early stage replaces tephri-phonolite. With the expansion comes an increase in the amount of eudialyte, which replaces part of arfvedsonite (Figure 11A) and form red-melanocratic kakortokite. Ultimately, an increase in the amount of eudialyte forms red kakortokite, of which an early stage is seen in the lower part of Figure 11A. The microstructures of the kakortokite veins in tephri-phonolite indicate that replacement of tephri-phonolite starts with arfvedsonite, followed by eudialyte, and it terminates with feldspar and, thus, they constitute a sequence in the order in which the minerals formed. Additionally, the microstructures suggest that the younger minerals in this sequence replace the older minerals, which as stated above, results in the formation of red-melanocratic kakortokite and red kakortokite, two typical members of the boundary zone.

The texture of the kakortokite veins in the tephri-phonolite does not reflect a magmatic infiltration of a kakortokite magma but suggests a chemical reaction between tephri-phonolite and a fluid phase. This assumption is supported by the pervasive replacement of tephri-phonolite, which locally occurs by disseminated eudialyte (Figure 11). Tephri-phonolite seems to act as a chemical barrier for the proposed alkaline fluid phase. Initially this causes a breakdown of tephri-phonolite and a simultaneous increase in the amount and grain size of arfvedsonite followed by precipitation of eudialyte. The breakdown of tephri-phonolite with a simultaneous growth of arfvedsonite will at least increase the fluid phase in Si, K, Zr and REE. This is presumably reflected in the later precipitation of eudialyte and K-feldspar. The proposed very different formation of kakortokite in, respectively, the lower boundary zone and in the upper part of the kakortokite stratigraphy is supported by the fact that the tiled structured perthite is missing in the lower boundary zone. The timing of the two metasomatic events is unresolved. There is no indication that the two metasomatic events occurred simultaneously nor occurred at different times.

The microstructure of the globular-structured kakortokite shows that the two types of perthite (lath and anhedral grains) have a different origin and that the anhedral, tiled structured, perthite appears as an original part of eudialyte-urtite. Therefore, the tiled perthite grains of white kakortokite can be regarded as a precursor mineral or xenocrysts in the metasomatic white kakortokite rock. A prominent aspect of the metasomatic process is the K-feldspar lath replacement of the precursor rock (eudialyte-urtite), which introduces the dominant feldspar laths of white kakortokite. The anhedral perthite shows no sign of replacement which indicates that the anhedral perthite most likely is in equilibrium with the fluid phase, which causes the metasomatic transformation. The presence of the anhedral perthite in the lower part of the LLK does not automatically imply that eudialyte-urtite has been a precursor in white kakortokite in this part of the stratigraphy.

The black kakortokite with its large content of arfvedsonite does not appear to have been affected by the metasomatic process, which indicates that arfvedsonite like the anhedral perthite seems to be in equilibrium with the fluid phase. The nature of precursors in the lower part of the stratigraphy and the conditions enclosing black kakortokite await further investigations.

Regardless of clarification of these matters, it turns out that the common view of overprinting the original ore by late magmatic to hydrothermal fluids leads to the enrichment of mineralization [42,43]. This applies likewise to the kakortokite REE mineralization. The eudialyte-urtite corresponds to the primary magmatic REE mineralization, which consists of disseminated eudialyte. The overprinting metasomatic event in the form of the massive K-feldspar replacement and the associated recrystallization turned eudialyte-urtite into white kakortokite. The enrichment of REE in white kakortokite compared to eudialyte-urtite is shown in Table 3. As REE predominantly occurs in eudialyte in both rocks, an enrichment of about 30% of REE in eudialyte has occurred during the metasomatism.

In the boundary zone of kakortokites, the tephri-phonolite represent the primary magmatic REE mineralization, averaging a TREE of 1371 ppm, including 21% heavy rare earth oxides (HREO) (Table 6). The REEs are hosted in the disseminated mineral rinkite. The reaction of the subsolidus hydrothermal fluid with tephri-phonolite changes the host mineral for REE from rinkite to eudialyte. Simultaneously, a significant conversion in texture takes place from a very fine-grained, allotriomorphic texture of tephri-phonolite to the medium grained, hypidiomorphic texture of kakortokite. An almost three-fold increase in TREE to 4055 ppm, including 28% HREO [23], is the result of the overprinting metasomatic event.

Where the boundary is between kakortokite formed by metasomatism of the eudialyte-urtite and the kakortokite formed by subsolidus hydrothermal reaction with tephri-phonolite cannot be determined with the current knowledge. Where the tephri-phonolite inclusions disappear, a lack of a clear repetitive kakortokite sequence occurs. This is due to massive K-feldspar replacement, which blurs the original structures and, thus, the possible boundary between the two types of formation.

In summary, the metasomatic events in the area of lower layered kakortokite begins with the transformation of eudialyte-urtite to white kakortokite and additionally with the subsolidus fluid reaction with tephri-phonolite, forming kakortokite of the lower boundary zone. In both cases, it is a widespread massive transformation of the original rock. This is followed by a widespread albitization previously described by [25], which specifically affects the K-feldspar and forms the perthite grains of the kakortokite sequence. The final metasomatic event described in detail by Karup-Møller et al., 2010 [44] is the transformation of eudialyte to catapleiite. This transformation varies enormously in the kakortokite sequence and shows completely altered grains close to unaffected grains. The alteration appears to be due to late fluids, which almost have preserved the bulk composition of the eudialyte but with a redistribution of the elements in newly formed extremely fine-grained minerals [44,45].

9. Summary

The lower layered kakortokite (LLK) of the Ilímaussaq complex consists of 29 exposed cyclic units consisting of black, red and white layers [4].

1. Features in the form of globular structures in the upper part of LLK shows that a precursor (eudialyte-urtite) was involved in the formation of white kakortokite.
2. Fine-grained inclusions of tephri-phonolite in the lower part of LLK support, rooted on textural and petrological data, that this part of the LLK is formed by a chemical reaction between a fluid phase and the underlying tephri-phonolite.
3. Textural evidence favors that the perthite laths of the eudialyte-urtite (precursor) is a porphyroblast and that the anhedral microcline in the matrix of the eudialyte-urtite is an original part of the matrix.
4. The anhedral microcline of the white kakortokite is probably a xenocryst, which indicates that white kakortokite most likely is a result of a metasomatic process.

5. The proposed different formation of kakortokite in the upper and lower part of the LLK is supported by the absence of the tiled structured microcline in the lower part of the LLK and that the precursor (eudialyte-urtite) is replaced by the fine-grained tephri-phonolite inclusions in the lower-most occurring kakortokite.
6. Overprinting metasomatic events enriched substantially the original REE mineralization. This supports the common view that multiple metasomatic events create the attractive REE grades in alkaline igneous complexes.
7. Several metasomatic events have contributed to the formation of the LLK. First, a massive transformation of eudialyte-urtite to white kakortokite in the upper part of the LLK and simultaneously or at a different time the subsolidus fluid reaction with tephri-phonolite forming the lower most part of the LLK. Then a widespread albitization previously described by [25] that specifically affected the K-feldspar and formed the perthite of LLK. Finally, as described by [42], a catapleiite replacement of eudialyte, which occurs locally, has almost preserved the bulk composition of eudialyte.

Author Contributions: Conceptualization, H.K.S. and G.B.; methodology, T.U.; investigation, H.K.S. and O.C.; data curation, H.K.S. and T.U.; writing—original draft preparation, H.K.S.; writing—review and editing, T.U., H.K.S., G.B. and O.C.; visualization, H.K.S. and T.U.; supervision, G.B.; project administration, H.K.S. and G.B. All authors have read and agreed to the published version of the manuscript.

Funding: This research received no external funding.

Data Availability Statement: Data are available from the corresponding author due to internal policy.

Acknowledgments: We would like to thank Anna Wingell and Erik Schønwandt for help in preparing the figures. Tanbreez Mining Greenland is thanked for permission to use and publish the company's data. We would like to thank three anonymous reviewers for their suggestions and comments that improved the structure and content of the paper.

Conflicts of Interest: The co-authors Hans Kristian Schønwandt and Greg Barnes are affiliated with the G.B. Barnes & Associates Mining company. The remaining authors declare that the research was conducted in the absence of any commercial or financial relationships that could be construed as a potential conflict of interest.

References

1. Sørensen, H. The agpaitic rocks-an overview. *Mineral. Mag.* **1997**, *61*, 485–498. [CrossRef]
2. Marks, M.A.W.; Markl, G. A global review on agpaitic rocks. *Earth-Sci. Rev.* **2017**, *173*, 229–258. [CrossRef]
3. Schønwandt, H.K.; Barnes, G.B.; Ulrich, T. A description of the world-class Rare earth element deposit, Tanbreez, South Greenland. In *Rare Earth Industry, Technology, Economic and Environmental Implications*; Lima, L.B., Filho, W.L., Eds.; Elsevier: Berlin/Heidelberg, Germany, 2016; pp. 73–85.
4. Bohse, H.; Brooks, C.K.; Kunzendorf, H. Field observations on the kakortokites of the Ilímaussaq intrusion, South Greenland. *Rapp. Grønl. Geol. Unders.* **1971**, *38*, 43. [CrossRef]
5. Bohse, H.; Andersen, S. Review of the stratigraphic divisions of kakortokite and Lujavrite in southern Ilímaussaq. *Rapp. Grønl. Geol. Unders.* **1981**, *103*, 53–62. [CrossRef]
6. Andersen, S.; Bohse, H.; Steenfelt, A. A geological section through the southern part of the Ilímaussaq intrusion South Greenland. *Rapp. Grønl. Geol. Unders.* **1981**, *103*, 39–42.
7. Upton, B.G.J. *Tectono-Magmatic Evolution of the Younger Gardar Southern Rift, South Greenland*; Geological Survey of Denmark and Greenland Bulletin; Danish Ministry of Climate, Energy and Building: Copenhagen, Denmark, 2013; Volume 29, p. 124.
8. Pfaff, K.; Krumrei, T.V.; Marks, M.A.W.; Venzel, T.; Rudolf, T.; Markl, G. Chemical and physical evolution of the "lower layered series" from the nepheline syenitic Ilímaussaq intrusion, South Greenland: Implication for the origin of magmatic layering in peralkaline felsic liquids. *Lithos* **2008**, *106*, 280–296. [CrossRef]
9. Hunt, E.J.; Finch, A.A.; Donalson, C.H. Layering in peralkaline magmas, Ilímaussaq Complex, S Greenland. *Lithos* **2017**, *268–271*, 1–15. [CrossRef]

10. Borst, A.M.; Friis, H.; Nielsen, T.F.D.; Waight, T.E. Bulk and melt evolution in agpaitic intrusions: Insight from compositional zoning in eudialyte, Ilímaussaq complex, South Greenland. *J. Petrol.* **2018**, *59*, 589–612. [CrossRef]
11. Andersen, S.; Bohse, H.; Steenfelt, A. *The Southern Part of the Ilímaussaq Complex, South Greenland, 1:20,000*; Geological Survey of Greenland; Ministry of the Environment: Copenhagen, Denmark, 1988.
12. Ferguson, J. Geology of the IlÍmaussaq alkaline intrusion, South Greenland: Description of map and structure. *Bull. Grønl. Geol. Unders.* **1964**, *39*, 82. [CrossRef]
13. Bailey, J.C.; Gwozdz, R.; Rose-Hansen, J.; Sørensen, H. Geochemical Overview of the IlÍmaussaq alkaline complex, South Greenland. In *The Ilímaussaq Alkaline Complex, South Greenland: Status of Mineralogical Research with New Results*; Sørensen, H., Ed.; Geology of Greenland Survey: Copenhagen, Denmark, 2001; Volume 190, pp. 35–53.
14. Krumrei, T.V.; Villa, L.A.; Marks, A.M.; Markl, G. A 40Ar/39Ar and U/Pb isotopic study of the IlÍmaussaq Complex, South Greenland: Implications for the 40K decay constant and the duration of magmatic Activity in a peralkaline complex. *Chem. Geol.* **2006**, *227*, 258–273. [CrossRef]
15. Marks, M.A.W.; Eggenkamp, H.G.M.; Atanasova, P.; Mundel, F.; Kümmel, S.; Hagen, M.; Wenzel, T.; Markl, G. Review on the Compositional Variation of Eudialyte-Group Minerals in the Ilímaussaq Complex (South Greenland). *Minerals* **2020**, *10*, 1011. [CrossRef]
16. Konnerup-Madsen, J.; Rose-Hansen, J.; Larsen, E. Hydrocarbon gas associated with alkaline igneous activity: Evidence from compositions of fluid inclusions. *Rapp. Grønl. Geol. Unders.* **1981**, *103*, 99–108.
17. Marks, M.A.W.; Markl, G. The Ilímaussaq alkaline complex, South Greenland. In *Layered Intru-Sions*; Charlier, B., Namur, O., Latypov, R., Tenger, C., Eds.; Springer Geology: Berlin/Heidelberg, Germany, 2015; pp. 649–691.
18. Ratschbacher, B.C.; Marks, M.A.W.; Bons, P.D.; Wenzel, T.; Markl, G. Emplacement and geochemical evolution of highly evolved syenites investigated by a combined structural and geochemical field study: The lujavrites of the Ilimaussaq complex, SW Greenland. *Lithos* **2015**, *231*, 62–76. [CrossRef]
19. Ferguson, J. The significance of the kakortokite in the evolution of the IlÍmaussaq intrusion, South Greenland. *Bull. Grønl. Geol. Unders.* **1970**, *89*, 193.
20. Sørensen, H. The IlÍmaussaq Alkaline Complex, South Greenland-An Overview of 200 Years of Research and an Outlook. *Meddelelser Om Grønland* **2006**, *45*, 70.
21. Ussing, N.V. Geology of the country around Julianehaab, Greenland. *Meddelelser Om Grønland* **1912**, *38*, 426.
22. Schønwandt, H.K.; Barnes, G.B.; Ulrich, T. Assimilation and extensive metasomatism of agpaitic rocks from the transitional layered kakortokite, Ilímaussaq intrusion, South Greenland. *Resour. Geol.* **2023**, *73*, e12320. [CrossRef]
23. Ussing, N.V. *Mineralogisk-petrografiske Undersøgelser af Grønlandske Nefelinsyeniter og beslægtede Bjærgarter*; B. Lunos kgl. hof-bogtrykkeri (F. Dreyer): Copenhagen, Denmark, 1894; Volume 14, pp. 1–124.
24. Smith, K.L.; McLarsen, A.C. TEM investigation of a microcline from a nepheline syenite. *Phys. Chem. Min.* **1983**, *10*, 69–76. [CrossRef]
25. Schønwandt, H.K.; Barnes, G.B.; Ulrich, T. Perthite in nepheline syenite from the kakortokite unit in the Ilímaussaq complex, South Greenland. *J. Geosci.* **2023**, *68*, 203–211. [CrossRef]
26. Mikhailova, J.A.; Ivanyuk, G.Y.; Kalashnikov, A.O.; Pakhomovsky, Y.A.; Bazai, A.V.; Yakovenchuk, V.N. Petrogenesis of eudialyte complex of the Lovozero Alkaline Massif (Kola Peninsula, Russia). *Minerals* **2019**, *9*, 581. [CrossRef]
27. Deer, W.A.; Howie, R.A.; Zussman, J. *Rock-Forming Minerals, Volume 4A, Framework Silicates, Feldspars*; The Geological Society: London, UK, 2001; p. 696.
28. Parsons, I. Feldspars defined and described: A pair of posters published by the Mineralogical Society. Sources and supporting information. *Mineral. Mag.* **2010**, *74*, 529–551. [CrossRef]
29. Dollase, W.A.; Thomas, W.M. The crystal chemistry of silica-rich, alkali-deficient nepheline. *Contrib. Mineral. Petrol.* **1978**, *13*, 57–81. [CrossRef]
30. Markl, G.; Marks, M.; Schwinn, G.; Sommer, H. Phase equilibrium constraints on intensive crystallization parameters of the Ilímaussaq Complex, South Greenland. *J. Petrol.* **2001**, *42*, 2231–2258. [CrossRef]
31. Hamilton, D.L. Nepheline as crystallization temperature indicator. *J. Petrol.* **1961**, *69*, 321–329. [CrossRef]
32. Leake, B.E. Nomenclature of amphiboles. *Am. Mineral.* **1978**, *63*, 1023–1052.
33. Morimoto, N. Nomenclature of pyroxenes. *Bull. De Mineral.* **1988**, *111*, 535–550.
34. Nielsen, J. Petrology and Mineralogy of Black Madonna from the Southern part of the Alkaline Ilimaussaq Complex, Southwest Greenland. Master's Thesis, Aarhus University, Aarhus, Denmark, 2016; p. 104.
35. Larsen, L.M. Clinopyroxenes and Coexisting Mafic Minerals from the Alkaline Ilímaussaq Intrusion, South Greenland. *J. Petrol.* **1976**, *17*, 258–290. [CrossRef]
36. Sørensen, H.; Bailey, J.C.; Kogarko, L.N.; Rose-Hansen, J.; Karup-Møller, S. Spheroidal structures in arfvedsonite lujavrite, Ilímaussaq alkaline complex, South Greenland—An example of macroscale liquid immiscibility. *Lithos* **2003**, *70*, 1–20. [CrossRef]

37. Sun, S.-S.; McDonough, W.F. Chemical and isotopic systematics of oceanic basalts: Implications for mantle composition and processes. *Geol. Soc. Lond. Spec. Publ.* **1989**, *42*, 313–345. [CrossRef]
38. Barker, A.J. *Introduction to Metamorphic Textures and Microstructures*; Stanley Thornes Ltd.: Cheltenham, UK, 1998; p. 263.
39. Verhoogen, J.; Turner, F.J.; Weiss, L.E.; Wahrhaftig, C.; Fyfe, W.S. *The Earth an Introduction to Physical Geology*; Holt, Reinhart and Winston, INC: New York, NY, USA, 1970; p. 745.
40. Féménias, O.; Coussaert, N.; Brassinnes, S.; Demaiffe, D. Emplacement processes and cooling history of layered cyclic unit II-7 from the Lovozero alkaline massif (Kola Peninsula, Russia). *Lithos* **2005**, *83*, 371–393. [CrossRef]
41. Schilling, J.; Wu, F.Y.; McCammon, C.; Wenzel, T.; Marks, M.A.W.; Pfaff, K.; Jacob, D.E.; Markl, G. The compositional variability of eudialyte-group minerals. *Mineral. Mag.* **2011**, *75*, 87–115. [CrossRef]
42. Dostal, J. Rare earth element deposits of alkaline igneous rocks. *Resources* **2017**, *6*, 34. [CrossRef]
43. Harmer, R.E.; Nex, P.A.M. Rare earth deposits of Africa. *Episodes* **2016**, *39*, 381–406. [CrossRef]
44. Karup-Møller, S.; Rose-Hansen, J.; Sørensen, H. Eudialyte decomposition minerals with new hitherto undescribed phases from the Ilímaussaq complex, South Greenland. *Bull. Geol. Soc. Den.* **2010**, *58*, 75–88. [CrossRef]
45. Borst, A.M.; Waight, T.; Smit, M.; Friis, H.; Nielsen, T. Alteration of eudialyte and implications for the REE, Zr and Nb resources of the layered kakortokites in the Ilímaussaq intrusion, South West Greenland. In Proceedings of the ERES2014: 1st European Rare Earth Resource Conference, Milos, Greece, 4–7 September 2014.